

Supplementary Document

A. Nature of oxygen speciation in N-A-S-H with varying Si/Al ratio

This section evaluates the influence of Si/Al ratio on the oxygen speciation in N-A-S-H. Figure 1(a) shows the distribution of bridging oxygen (BO), non-bridging oxygen (NBO) and tricluster oxygen (TO) in N-A-S-H. Significant difference is observed with the percentage of BO in NASH1 compared to NASH2 and NASH3. Similarly, for the case of NBO in NASH1 compared to NASH2 and NASH3. This difference can be attributed to the availability of Na to interact with Si-O network leading to Si-O-Na interaction where more SiO_2 content favors the interaction. Given the fact that the interaction of Na and water to the network is itself complicated, it is difficult to draw any conclusion based on BO and NBO as both Si and Al are network formers.

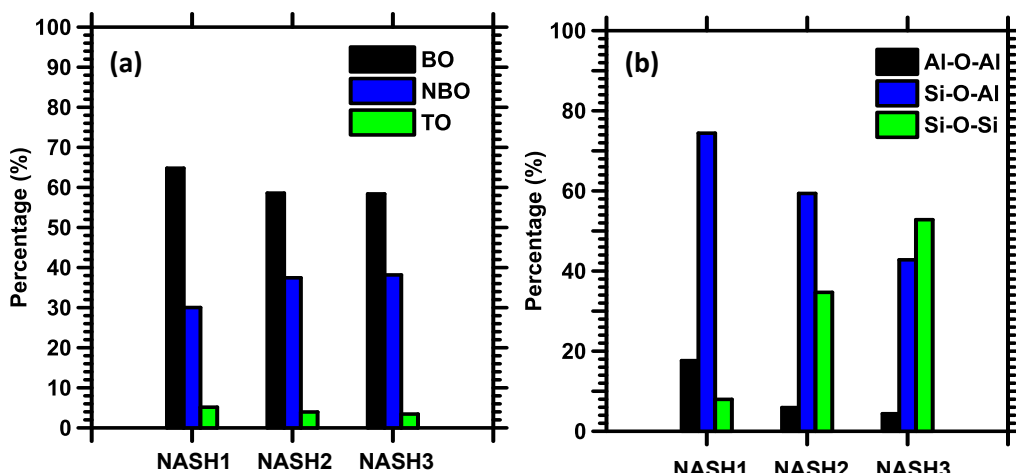


Figure 1: (a) Nature of oxygen speciation, and (b) Different BO components in N-A-S-H

However, clear difference is visible when the BO is decomposed into its components where the content of Si-O-Si increases with increase in Si/Al ratio (as it is expected) as shown in Figure 1(b). On the contrary, the content of Si-O-Al and Al-O-Al decreases with increase in Si/Al ratio. Nevertheless, the majority of the network structure is formed by Si-O-Si and Si-O-Al bonds. The effect of decreasing BO also can be observed from the medium-range order via ring structure. Where it is shown that smaller rings were prominent with NASH3 and NASH2 and the least with NASH1. A trace of TO is also observed in the structure. The presence of TO indicates the defect in the glass structure. Such presence of TO is also observed in MD simulation of NAS glass¹. Figure 1(b) shows the fraction of Si-O-Si, Si-O-Al and Al-O-Al in the BO. Figure 2 shows the representative view of Si-O-Si, Si-O-Al, Al-O-Al, Si-O-H, Al-O-H, and H₂Ow. Table 1 exhibits the quantification of Si-[O,Ow]-H, Al-[O,Ow]-H, Na-[O,Ow]-H, and H-Ow-H in the NASH

structure with different Si/Al compositions. It is clearly evident that more number of Si-[O,Ow]-H is observed for NASH3 where the content of SiO_2 is high.

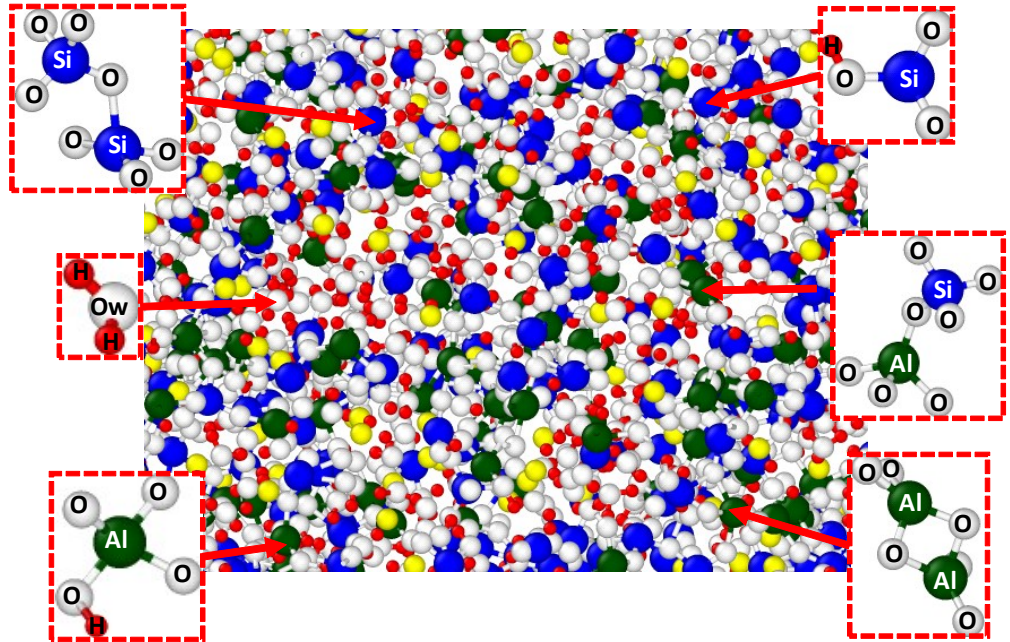


Figure 2: Representative atomic structure of NASH3 showing the presence of Si-O-Si, Si-O-Al, Al-O-Al, Si-O-H, Al-O-H, and H_2Ow . (Si: Navy blue, Al: Green, O & Ow: White, H: Red and Na: Yellow).

Table 1: Quantification of different bond formation obtained by ReaxFF due to dissociation of water

	Si-[O,Ow]-H	Al-[O,Ow]-H	Na-[O,Ow]-H	H-Ow-H
NASH1 (Si/Al=1)	31.89%	15.85%	20.55%	31.71%
NASH2 (Si/Al=2)	33.01%	5.31%	11.75%	34.53%
NASH3 (Si/Al=3)	42.73%	4.67%	14.13%	20.77%

B. Diffusion coefficient of water in N-A-S-H

This section describes the linear correlation between mean squared displacement (MSD) of water molecules with respect to time evolution as shown in Figure 3. Good linear variations of MSD are observed between 3 ns to 8 ns. Henceforth, this range has been used to compute the diffusion coefficient of water molecules for all the cases in this paper with respect to different Si/Al ratios and different water contents.

Similar approach is also applied to compute the diffusion coefficient of sodium ions in the N-A-S-H structure.

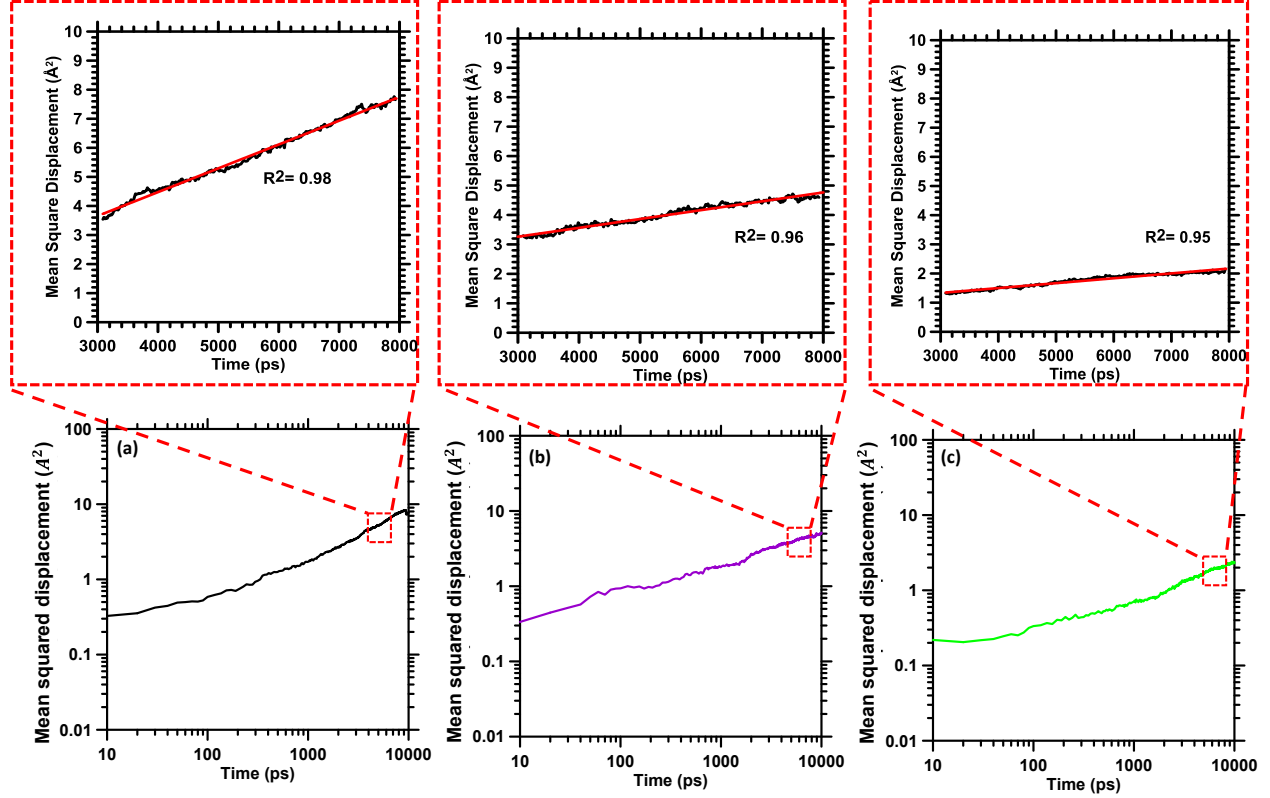


Figure 3: MSD plot of water with time for (a) NASH1 (Si/Al=1), (b) NASH2 (Si/Al=2), and (c) NASH3 (Si/Al=3) along with fitting curve and its R^2 values (from 3 ns to 8 ns)

C. Pair distribution function and structure factor of NASH structures with different water contents

In this section, the structural characteristic of N-A-S-H structure with different water contents is validated with the experimental data. N-A-S-H structures with 5%, 10%, 15%, and 20% water content are denoted as NASH-5, NASH-10, NASH-15, and NASH-20, respectively. Figure 4(a) shows the broadened pair distribution functions (PDFs) obtained for N-A-S-H structures with different water contents using the methodology explained in section 2.3 of the main article. Three distinct peaks are observed from PDF. The initial peak at 1.0 \AA corresponds to the D-O interaction (where D refers to deuterium which is equivalent to O-H bond). The second peak at 1.62 \AA is a combination of Si-O and Al-O interactions. The other peak value at 2.6 \AA corresponds to the O-O interactions. It is observed the constructed N-A-S-H structures especially for NASH with water content equal to 15-20% are in excellent agreement with experimental data signifying the viability of the constructed structures in terms of short-range order.

With a view to evaluate the viability of the constructed N-A-S-H structures in the medium-range order, the neutron structure factor, computed for the constructed molecular structures, is plotted against the experimental data as shown in Figure 4(b). It is evident that the structure factor for NASH contains four distinct peaks, the position of which correlates very well with the experimental observations. This indicates that the N-A-S-H structure with water content in the range 15-20% represent the experimental data effectively and hence presence of such water content in N-A-S-H is likely to be realistic. Similar observations are reported experimentally in the literature.

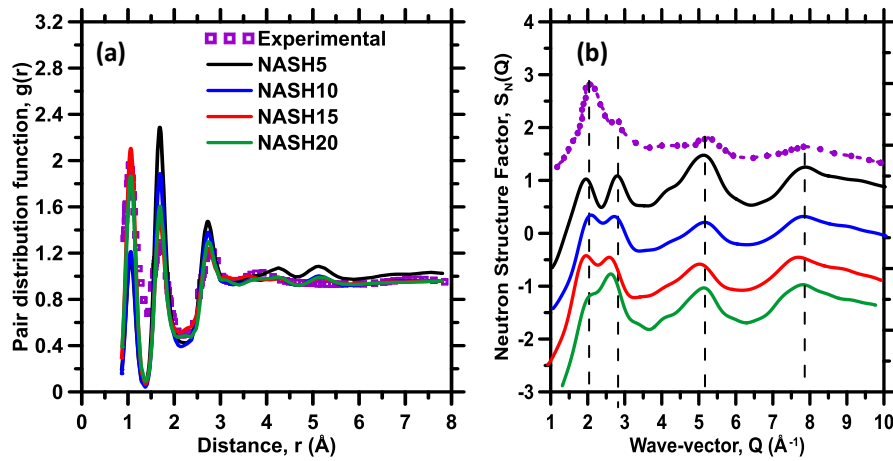


Figure 4: (a) Pair distribution function and (b) structure factor of the N-A-S-H model with different water content, compared with the experimental data².

D. Influence of water content on the partial pair distribution function of different interactions in N-A-S-H

The local structure of the N-A-S-H gel with different water contents is investigated in this section by computing the partial PDFs. Here, the discussion solely focuses on the interactions of water and alkali species such as Na–O, Na–Ow, O–O, O–Ow, Ow–Ow, O–H, and Ow–H. Figure 5(a) shows the partial PDF for Na–O interactions in NASH with different water contents. From Figure 5(a) three peaks are observed. The first peak at 2.30–2.35 Å corresponds to the interaction of Na with non-bridging oxygen (NBO), which is also observed both numerically and experimentally^{3–7}, and the second peak at 2.55 Å corresponds to the interaction of Na with bridging oxygen (BO)⁴. However, the second peaks are not prevalent for the case when water is fully equilibrated which is evident for all Si/Al ratio equal to 1, 2 and 3 (as shown in Figure 4 in the main article). This implies that the second peaks could be correlated with the equilibration of the structure rather than the nature of the interaction between Na with NBO. This indicates that the parameterization of ReaxFF recognizes two different sodium-oxygen environments effectively. Figure

5(b) shows the interaction of Na with water in the N-A-S-H structure. Here two peaks are observed between 2-2.35 Å. Presence of such dual peak can be explained from the nature of Na around the vicinity of water molecules, where the coordination of Na shows variation between 1 to 6⁴. The average coordination of Na⁺ with Ow and O are found to be 5.3, 5.8, 5.8, and 5.5 for 5%, 10%, 15%, and 20% water content, respectively. Experimentally, the coordination of Na around oxygen in aqueous solution lies in the range 4.3-6.2 Å⁴⁻⁷. This shows the consistency of the MD simulations with the experimental observations.

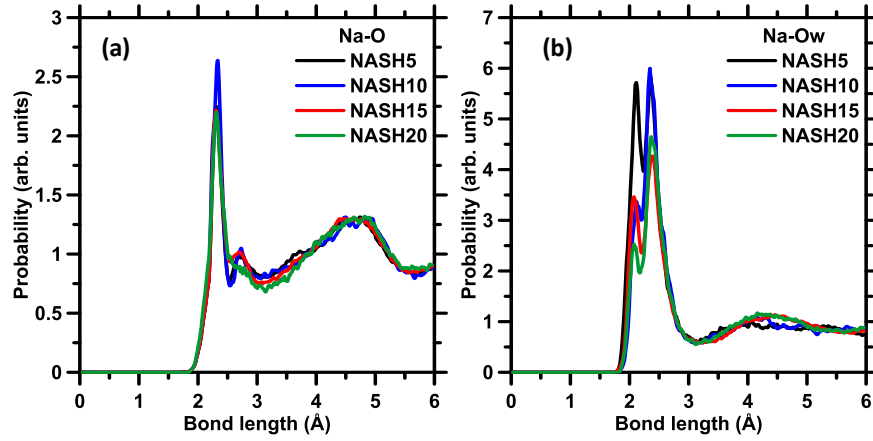


Figure 5: Partial PDF of (a) Na-O, and (b) Na-Ow for NASH structure with different water content.

Figure 6(a) shows the partial PDF of tetrahedral oxygen in N-A-S-H with varying water content. The first peak at 2.73-2.75 Å is present in all the structures irrespective of water content and it corresponds to the O-O bond³. Such results suggest that the O-O bond belonging to the ring structure is stable irrespective of the water content.

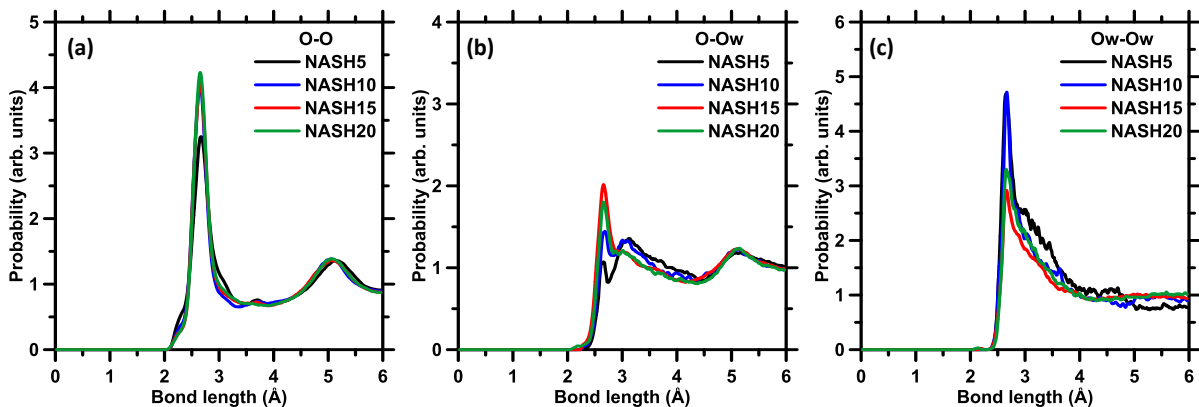


Figure 6: Partial PDF of (a) O-O, (b) O-Ow, and (c) Ow-Ow where O (represent to oxygen connected to polyhedral structure) and Ow (represent oxygen in water) for NASH gel with 5% (NASH5), 10% (NASH10), 15% (NASH15), and 20% (NASH20) water content, respectively.

Figure 6(b) shows the influence of water content on the of O–Ow interactions where three distinct peaks are observed (2.75 \AA , 3.3 \AA and 5.3 \AA). While the first peak at 2.75 \AA indicates interaction of O with the first neighboring atom (first coordination shell between oxygen atoms) in water (Ow), the third peak at 5.3 \AA corresponds to second neighbor interactions. The first peak at 2.75 \AA is also present in case of O–O and Ow–Ow bonds as shown in Figure 6, and previous observations^{8–11}. The second peak observed at 3.3 \AA is due to local interaction between the O and Ow present in the hydrated glass structure with variation of water content. The second peak at 3.3 \AA weakens with increasing water content. Similar observations are shown for hydrated disordered aluminosilicates in the literature⁸. Irrespective of the water content, the peak at 5.3 \AA corresponding to second neighbor interaction remains unaffected. Figure 6(c) shows the partial PDF of Ow–Ow interaction in N-A-S-H. The peak at 2.76\AA^{12} is observed for all the cases. However, the second peaks are not prevalent in this Ow–Ow interaction, which are attributed to the confined nature of water molecules⁸.

In order to get insight on the behavior of water in the disordered structure, a water bulk system is simulated using the same ReaxFF. Note that a density of approximately 0.94 g/cm^3 is obtained for bulk water using this potential, which is consistent with the value reported in the literature^{13–15}. Figure 7(a-b) shows the partial PDF for the O–H, and Ow–H bonds. Both O–H and Ow–H bonds do not show any significant change in bond lengths irrespective of water content. In case of Ow–H interaction, it is observed that the behavior of the bonds for gel structure is similar to that of bulk water. Ow–H interaction in bulk water is consistent with the behavior reported in the literature^{12,16}.

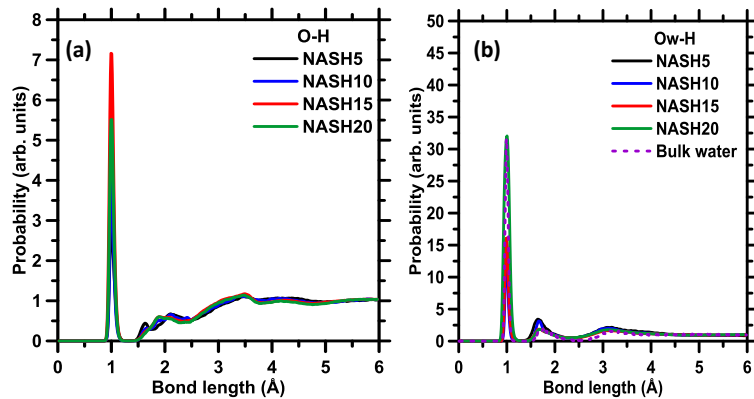


Figure 7: Partial PDF of (a) O–H, and (b) Ow–H (hydroxyl) where Ow (represent oxygen in water), and H (represent hydrogen in water) for NASH gel with 5% (NASH5), 10% (NASH10), 15% (NASH15), and 20% (NASH20) water content respectively. For Ow–H, a partial PDF from bulk water is also plotted.

E. Reactive Forcefield for N-A-S-H

Reactive MD-force field: c/h/o/water/Al/Si/Fe (Pitman et al., JACS 2012)

39 ! Number of general parameters
50.0000 !Overcoordination parameter
9.5469 !Overcoordination parameter
1.6725 !Valency angle conjugation parameter
1.7224 !Triple bond stabilisation parameter
6.8702 !Triple bond stabilisation parameter
60.4850 !C2-correction
1.0588 !Undercoordination parameter
4.6000 !Triple bond stabilisation parameter
12.1176 !Undercoordination parameter
13.3056 !Undercoordination parameter
-55.1978 !Triple bond stabilization energy
0.0000 !Lower Taper-radius
10.0000 !Upper Taper-radius
2.8793 !Not used
33.8667 !Valency undercoordination
6.0891 !Valency angle/lone pair parameter
1.0563 !Valency angle
2.0384 !Valency angle parameter
6.1431 !Not used
6.9290 !Double bond/angle parameter
0.3989 !Double bond/angle parameter: overcoord
3.9954 !Double bond/angle parameter: overcoord
-2.4837 !Not used
5.7796 !Torsion/BO parameter
10.0000 !Torsion overcoordination
1.9487 !Torsion overcoordination
-1.2327 !Conjugation 0 (not used)
2.1645 !Conjugation
1.5591 !vdWaals shielding
0.1000 !Cutoff for bond order (*100)
1.7602 !Valency angle conjugation parameter
0.6991 !Overcoordination parameter
50.0000 !Overcoordination parameter
1.8512 !Valency/lone pair parameter
0.5000 !Not used
20.0000 !Not used
5.0000 !Molecular energy (not used)
0.0000 !Molecular energy (not used)
0.7903 !Valency angle conjugation parameter
9 ! Nr of atoms; cov.r; valency;a.m;Rvdw;Evdw;gammaEEM;cov.r2;#
alfa;gammavdW;valency;Eunder;Eover;chiEEM;etaEEM;n.u.
cov r3;Elp;Heat inc.;n.u.;n.u.;n.u.;n.u.
ov/un;val1;n.u.;val3,vval4

C	1.3817	4.0000	12.0000	1.8903	0.1838	0.9000	1.1341	4.0000	
	9.7559	2.1346	4.0000	34.9350	79.5548	5.9666	7.0000	0.0000	
	1.2114	0.0000	202.6057	8.9539	34.9289	13.5366	0.8563	0.0000	
	-2.8983	2.5000	1.0564	4.0000	2.9663	1.2000	0.2000	13.0000	
H	0.8930	1.0000	1.0080	1.3550	0.0930	0.8203	-0.1000	1.0000	
	8.2230	33.2894	1.0000	0.0000	121.1250	3.7248	9.6093	1.0000	
	-0.1000	0.0000	61.6606	3.0408	2.4197	0.0003	1.0698	0.0000	
	-19.4571	4.2733	1.0338	1.0000	2.8793	1.0000	0.2000	12.0000	
O	1.2450	2.0000	15.9990	2.3890	0.1000	1.0898	1.0548	6.0000	
	9.7300	13.8449	4.0000	37.5000	116.0768	8.5000	8.3122	2.0000	
	0.9049	0.4056	59.0626	3.5027	0.7640	0.0021	0.9745	0.0000	
	-3.5500	2.9000	1.0493	4.0000	2.9225	1.3000	0.2000	13.0000	
Fe	1.9506	3.0000	55.8450	2.0308	0.1274	0.7264	-1.0000	3.0000	
	11.0534	2.2637	3.0000	0.0000	18.3725	1.2457	7.3021	0.0000	
	-1.2000	0.0000	66.4838	30.0000	1.0000	0.0000	0.8563	0.0000	
	-16.2040	2.7917	1.0338	6.0000	2.5791	1.3000	0.2000	13.0000	
Cl	1.7140	1.0000	35.4500	1.9139	0.2000	0.3837	-1.0000	7.0000	
	11.5345	10.1330	1.0000	0.0000	0.0000	9.9614	6.5316	0.0000	
	-1.0000	3.5750	143.1770	6.2293	5.2294	0.1542	0.8563	0.0000	
	-10.2080	2.9867	1.0338	6.2998	2.5791	1.3000	0.2000	13.0000	
Si	2.1932	4.0000	28.0600	1.8951	0.1737	0.8112	1.2962	4.0000	
	11.3429	5.2054	4.0000	21.7115	139.9309	4.0081	5.7104	0.0000	
	-1.0000	0.0000	128.2031	9.0751	23.8188	0.8381	0.8563	0.0000	
	-4.1684	2.0754	1.0338	4.0000	2.5791	1.4000	0.2000	13.0000	
Al	2.1967	3.0000	26.9820	2.3738	0.2328	0.4558	-1.6836	3.0000	
	9.4002	3.9009	3.0000	0.0076	16.5151	1.6032	6.7003	0.0000	
	-1.0000	0.0000	78.4675	20.0000	0.2500	0.0000	0.8563	0.0000	
	-23.1826	1.5000	1.0338	8.0000	2.5791	1.4000	0.2000	13.0000	
Ca	1.9927	2.0000	40.0870	2.7005	0.1848	0.7939	1.0000	2.0000	
	10.6123	27.5993	3.0000	38.0000	0.0000	-1.9372	6.5275	0.0000	
	-1.3000	0.0000	220.0000	49.9248	0.3370	0.0000	0.0000	0.0000	
	-2.0000	4.0000	1.0564	6.2998	2.9663	1.4000	0.0100	13.0000	
Na	1.8000	1.0000	22.9898	2.8270	0.1872	0.4000	-1.0000	1.0000	
	10.0000	2.5000	1.0000	0.0000	0.0000	-1.2155	6.8737	0.0000	
	-1.0000	0.0000	23.0445	100.0000	1.0000	0.0000	0.8563	0.0000	
	-2.5000	3.9900	1.0338	8.0000	2.5791	1.4000	0.0100	13.0000	
34	! Nr of bonds; Edis1;LPpen;n.u.;pbe1;pbo5;13corr;pbo6 pbe2;pbo3;pbo4;Etrip;pbo1;pbo2;ovcorr								
1	1	158.2004	99.1897	78.0000	-0.7738	-0.4550	1.0000	37.6117	0.4147
		0.4590	-0.1000	9.1628	1.0000	-0.0777	6.7268	1.0000	0.0000
1	2	169.4760	0.0000	0.0000	-0.6083	0.0000	1.0000	6.0000	0.7652
		5.2290	1.0000	0.0000	1.0000	-0.0500	6.9136	0.0000	0.0000
2	2	153.3934	0.0000	0.0000	-0.4600	0.0000	1.0000	6.0000	0.7300
		6.2500	1.0000	0.0000	1.0000	-0.0790	6.0552	0.0000	0.0000
1	3	164.4303	82.6772	60.8077	-0.3739	-0.2351	1.0000	10.5036	1.0000
		0.4475	-0.2288	7.0250	1.0000	-0.1363	4.8734	0.0000	0.0000
3	3	142.2858	145.0000	50.8293	0.2506	-0.1000	1.0000	29.7503	0.6051
		0.3451	-0.1055	9.0000	1.0000	-0.1225	5.5000	1.0000	0.0000

2	3	160.0000	0.0000	0.0000	-0.5725	0.0000	1.0000	6.0000	0.5626
		1.1150	1.0000	0.0000	0.0000	-0.0920	4.2790	0.0000	0.0000
1	4	133.0514	0.0000	0.0000	1.0000	-0.3000	1.0000	36.0000	0.0673
		0.2350	-0.3500	15.0000	1.0000	-0.1143	4.5217	1.0000	0.0000
2	4	105.0054	0.0000	0.0000	-0.0717	0.0000	0.0000	6.0000	0.0505
		0.1000	1.0000	0.0000	1.0000	-0.1216	4.5062	0.0000	0.0000
3	4	65.7713	0.0000	0.0000	0.1366	-0.3000	1.0000	36.0000	0.0494
		0.9495	-0.3500	15.0000	1.0000	-0.0555	7.9897	1.0000	0.0000
4	4	38.7471	0.0000	0.0000	0.3595	-0.2000	0.0000	16.0000	0.2749
		1.0000	-0.2000	15.0000	1.0000	-0.0771	6.4477	0.0000	0.0000
2	5	109.1686	0.0000	0.0000	-0.1657	-0.2000	0.0000	16.0000	1.2500
		2.8463	-0.2000	15.0000	1.0000	-0.1111	5.2687	0.0000	0.0000
3	5	0.0000	0.0000	0.0000	0.5000	-0.2000	0.0000	16.0000	0.5000
		1.0001	-0.2000	15.0000	1.0000	-0.1000	10.0000	0.0000	0.0000
4	5	0.0000	0.0000	0.0000	0.2500	-0.2000	0.0000	16.0000	0.5000
		0.5000	-0.2000	15.0000	1.0000	-0.2000	10.0000	0.0000	0.0000
5	5	0.2500	0.0000	0.0000	0.1803	-0.2000	0.0000	16.0000	0.3356
		0.9228	-0.2000	15.0000	1.0000	-0.1178	5.6715	0.0000	0.0000
1	6	0.0000	0.0000	0.0000	-0.6528	-0.3000	0.0000	36.0000	0.5000
		10.0663	-0.3500	25.0000	1.0000	-0.1000	10.0000	0.0000	0.0000
2	6	250.0000	0.0000	0.0000	-0.7128	0.0000	1.0000	6.0000	0.1186
		18.5790	1.0000	0.0000	1.0000	-0.0731	7.4983	0.0000	0.0000
3	6	261.9074	5.9533	0.0000	-0.6223	-0.3000	1.0000	36.0000	0.7275
		10.1541	-0.2366	29.7817	1.0000	-0.1083	8.5924	6.0658	0.0000
6	6	70.9120	54.0531	30.0000	0.4931	-0.3000	1.0000	16.0000	0.0392
		0.2476	-0.8055	7.1248	1.0000	-0.1009	8.7229	0.0000	0.0000
1	7	0.0000	0.0000	0.0000	-0.6528	-0.3000	0.0000	36.0000	0.5000
		10.0663	-0.3500	25.0000	1.0000	-0.1000	10.0000	0.0000	0.0000
2	7	92.8579	0.0000	0.0000	-0.6528	-0.3000	0.0000	36.0000	0.1551
		10.0663	-0.3500	25.0000	1.0000	-0.0842	7.1758	0.0000	0.0000
3	7	228.4876	0.0000	0.0000	-0.8524	-0.3000	0.0000	36.0000	0.1252
		0.4016	-0.3500	25.0000	1.0000	-0.1750	5.2102	0.0000	0.0000
6	7	0.0000	0.0000	0.0000	1.0000	0.3000	0.0000	26.0000	1.0000
		0.5000	0.0000	12.0000	1.0000	-0.2000	10.0000	0.0000	0.0000
7	7	34.0777	0.0000	0.0000	0.4832	-0.3000	0.0000	16.0000	0.5154
		6.4631	-0.4197	14.3085	1.0000	-0.1463	6.1608	0.0000	0.0000
2	8	0.0000	0.0000	0.0000	-0.0203	-0.1418	1.0000	13.1260	0.0230
		8.2136	-0.1310	0.0000	1.0000	-0.2692	6.4254	0.0000	24.4461
3	8	50.8757	0.0000	43.3991	1.0000	-0.3000	1.0000	36.0000	0.0025
		0.7609	-0.2500	12.0000	1.0000	-0.0515	8.9041	1.0000	24.4461
6	8	0.0000	0.0000	0.0000	0.5000	-0.3000	1.0000	16.0000	0.5000
		0.5000	-0.2500	15.0000	1.0000	-0.1000	9.0000	0.0000	0.0000
7	8	0.0000	0.0000	0.0000	0.5000	-0.3000	1.0000	16.0000	0.5000
		0.5000	-0.2500	15.0000	1.0000	-0.1000	9.0000	0.0000	0.0000
8	8	36.9494	0.0000	0.0000	-0.0412	-0.2000	0.0000	16.0000	0.3233
		0.3708	-0.2000	10.0000	1.0000	-0.0822	4.2104	0.0000	0.0000
2	9	0.0000	0.0000	0.0000	-1.0000	-0.3000	1.0000	36.0000	0.7000
		10.1151	-0.3500	25.0000	1.0000	-0.1053	8.2003	1.0000	0.0000

3 9 48.5875 0.0000 0.0000 -0.0157 -0.3000 1.0000 36.0000 0.5922
 6.8772 -0.3500 25.0000 1.0000 -0.0630 7.8526 1.0000 0.0000
 6 9 0.1000 0.0000 0.0000 0.2500 -0.5000 1.0000 35.0000 0.6000
 0.5000 -0.5000 20.0000 1.0000 -0.2000 10.0000 1.0000 0.0000
 7 9 0.0000 0.0000 0.0000 0.5000 -0.3000 1.0000 16.0000 0.5000
 0.5000 -0.2500 15.0000 1.0000 -0.1000 9.0000 0.0000 0.0000
 8 9 0.0000 0.0000 0.0000 0.5000 -0.3000 1.0000 16.0000 0.5000
 0.5000 -0.2500 15.0000 1.0000 -0.1000 9.0000 0.0000 0.0000
 9 9 60.0000 0.0000 0.0000 -0.3458 0.3000 0.0000 25.0000 0.2477
 2.4578 -0.4000 12.0000 1.0000 -0.0513 4.5180 0.0000 0.0000
 24 ! Nr of off-diagonal terms; Ediss;Ro;gamma;rsigma;rpi;rpi2
 1 2 0.1239 1.4004 9.8467 1.1210 -1.0000 -1.0000
 2 3 0.0283 1.2885 10.9190 0.9215 -1.0000 -1.0000
 1 3 0.1345 1.8422 9.7725 1.2835 1.1576 1.0637
 1 4 0.1358 1.8293 10.0425 1.6096 -1.0000 -1.0000
 2 4 0.0640 1.6974 11.5167 1.3517 -1.0000 -1.0000
 3 4 0.0846 1.4284 10.0808 1.8339 -1.0000 -1.0000
 2 5 0.0568 1.6740 9.6297 1.2200 -1.0000 -1.0000
 3 5 0.1927 2.2551 11.2308 -1.0000 -1.0000 -1.0000
 4 5 0.1500 2.1500 11.0000 -1.0000 -1.0000 -1.0000
 1 6 0.2000 1.9000 12.0000 -1.0000 -1.0000 -1.0000
 2 6 0.2000 1.5207 12.9535 1.2125 -1.0000 -1.0000
 3 6 0.2000 1.9048 10.8374 1.7163 1.2444 -1.0000
 1 7 0.2000 1.9000 12.0000 -1.0000 -1.0000 -1.0000
 2 7 0.0564 1.4937 12.0744 1.7276 -1.0000 -1.0000
 3 7 0.1651 1.8998 11.2212 1.5416 -1.0000 -1.0000
 6 7 0.0216 1.5025 11.8792 -1.0000 -1.0000 -1.0000
 1 8 0.1000 1.9000 11.5000 -1.0000 -1.0000 -1.0000
 2 8 0.0100 1.6000 13.2979 -1.0000 -1.0000 -1.0000
 3 8 0.0955 1.7587 11.9417 1.9052 -1.0000 -1.0000
 6 8 0.1000 1.9000 11.0000 -1.0000 -1.0000 -1.0000
 7 8 0.1000 1.9000 11.0000 -1.0000 -1.0000 -1.0000
 3 9 0.1574 1.5000 11.8005 1.5685 -1.0000 -1.0000
 6 9 0.1315 2.0482 17.5616 -1.0000 -1.0000 -1.0000
 7 9 0.1315 2.0482 17.5616 -1.0000 -1.0000 -1.0000
 69 ! Nr of angles;at1;at2;at3;Thetao,o;ka;kb;pv1;pv2
 1 1 1 59.0573 30.7029 0.7606 0.0000 0.7180 6.2933 1.1244
 1 1 2 65.7758 14.5234 6.2481 0.0000 0.5665 0.0000 1.6255
 2 1 2 70.2607 25.2202 3.7312 0.0000 0.0050 0.0000 2.7500
 1 2 2 0.0000 0.0000 6.0000 0.0000 0.0000 0.0000 1.0400
 1 2 1 0.0000 3.4110 7.7350 0.0000 0.0000 0.0000 1.0400
 2 2 2 0.0000 27.9213 5.8635 0.0000 0.0000 0.0000 1.0400
 1 1 3 53.9517 7.8968 2.6122 0.0000 3.0000 58.6562 1.0338
 3 1 3 76.9627 44.2852 2.4177 -25.3063 1.6334 -50.0000 2.7392
 2 1 3 65.0000 16.3141 5.2730 0.0000 0.4448 0.0000 1.4077
 1 3 1 72.6199 42.5510 0.7205 0.0000 2.9294 0.0000 1.3096
 1 3 3 81.9029 32.2258 1.7397 0.0000 0.9888 68.1072 1.7777
 3 3 3 80.7324 30.4554 0.9953 0.0000 3.0000 50.0000 1.0783

1	3	2	70.1101	13.1217	4.4734	0.0000	0.8433	0.0000	3.0000
2	3	3	75.6935	50.0000	2.0000	0.0000	1.0000	0.0000	1.1680
2	3	2	85.8000	9.8453	2.2720	0.0000	2.8635	0.0000	1.5800
1	2	3	0.0000	25.0000	3.0000	0.0000	1.0000	0.0000	1.0400
3	2	3	0.0000	15.0000	2.8900	0.0000	0.0000	0.0000	2.8774
2	2	3	0.0000	8.5744	3.0000	0.0000	0.0000	0.0000	1.0421
1	4	1	29.1655	3.3035	0.2000	0.0000	1.1221	0.0000	1.0562
1	1	4	59.8697	2.8115	1.9262	0.0000	0.7602	0.0000	1.4056
1	4	4	25.4591	15.9430	0.9664	0.0000	2.2242	0.0000	1.1088
4	1	4	88.6279	26.0015	1.0328	0.0000	0.2361	0.0000	2.0576
2	1	4	47.3695	16.9204	4.1052	0.0000	0.1000	0.0000	1.0050
2	4	2	34.1965	6.6782	6.5943	0.0000	1.3895	0.0000	1.5365
2	2	4	0.1000	30.0000	3.4094	0.0000	2.4379	0.0000	1.5166
4	2	4	0.0000	8.2994	5.7832	0.0000	2.9873	0.0000	1.7716
2	4	4	21.2590	6.5954	0.9951	0.0000	2.8006	0.0000	1.0000
2	4	4	180.0000	-6.9970	24.3956	0.0000	0.7878	0.0000	1.3672
1	3	4	90.0000	12.8684	1.4601	0.0000	0.8757	0.0000	1.0000
3	1	4	18.8567	24.3753	3.9647	0.0000	0.1000	0.0000	1.5314
3	4	3	79.7335	0.0100	0.1392	0.0000	0.4968	0.0000	2.1948
4	3	4	57.6787	4.8566	2.5768	0.0000	0.7552	0.0000	1.0000
2	3	4	59.4556	10.2025	0.7481	0.0000	1.4521	0.0000	1.0000
3	3	4	73.6721	32.6330	1.7223	0.0000	1.0221	0.0000	1.4351
3	4	4	65.7545	5.6268	4.0645	0.0000	1.7794	0.0000	2.6730
3	2	4	0.0000	4.6026	2.5343	0.0000	0.7284	0.0000	1.1051
2	4	3	34.0653	20.1868	4.7461	0.0000	0.1000	0.0000	1.6752
3	2	5	0.0000	0.0100	0.5211	0.0000	0.0000	0.0000	1.3859
6	6	6	78.5339	36.4328	1.0067	0.0000	0.1694	0.0000	1.6608
2	6	6	77.2616	5.0190	7.8944	0.0000	4.0000	0.0000	1.0400
2	6	2	75.7983	14.4132	2.8640	0.0000	4.0000	0.0000	1.0400
3	6	6	90.6812	31.1846	4.4543	0.0000	0.5073	0.0000	2.1809
2	6	3	73.6998	40.0000	1.8782	0.0000	4.0000	0.0000	1.1290
3	6	3	80.1361	36.2368	0.9504	0.0000	0.2624	0.0000	2.0787
6	3	6	80.4450	6.0739	1.7731	0.0000	3.2548	0.0000	1.0422
2	3	6	86.7611	7.1742	1.4013	0.0000	1.4999	0.0000	1.0400
3	3	6	103.4529	26.9589	1.3470	0.0000	1.7728	0.0000	1.3091
2	2	6	0.0000	47.1300	6.0000	0.0000	1.6371	0.0000	1.0400
6	2	6	0.0000	27.4206	6.0000	0.0000	1.6371	0.0000	1.0400
3	2	6	0.0000	5.0000	1.0000	0.0000	1.0000	0.0000	1.2500
3	2	7	0.0000	4.2750	1.0250	0.0000	1.3750	0.0000	1.4750
2	2	7	0.0000	3.0000	1.0000	0.0000	1.0000	0.0000	1.2500
7	2	7	0.0000	20.2391	0.1328	0.0000	2.9860	0.0000	1.0870
2	3	7	88.1144	13.2143	1.5068	0.0000	3.0000	0.0000	1.0100
3	3	7	34.4326	25.9544	5.1239	0.0000	2.7500	0.0000	1.7141
7	3	7	21.6945	20.0000	4.0000	0.0000	0.6619	0.0000	1.9714
2	7	2	67.4229	4.5148	5.9702	0.0000	3.0000	0.0000	2.6879
2	7	3	41.8108	17.3800	2.6618	0.0000	0.7372	0.0000	1.0100
3	7	3	49.1145	11.8902	2.1383	0.0000	3.0000	0.0000	1.4790
2	7	7	180.0000	-26.7860	7.3549	0.0000	1.0000	0.0000	1.0252

2 7 7 78.2279 37.6504 0.4809 0.0000 1.0000 0.0000 2.9475
 6 3 7 16.5023 0.0100 2.7027 0.0000 1.0000 0.0000 1.0000
 3 6 7 88.2703 0.3954 0.2500 0.0000 0.5000 0.0000 2.1060
 3 7 6 83.8306 0.3712 0.2500 0.0000 0.5000 0.0000 2.1153
 3 8 3 1.0000 4.9611 2.4541 0.0000 0.5754 0.0000 1.0000
 8 3 8 9.5066 4.2640 3.1438 0.0000 1.9819 0.0000 1.6463
 2 3 8 51.3829 2.5000 0.2500 0.0000 0.0500 0.0000 1.0000
 3 3 8 70.0000 25.0000 1.0000 0.0000 1.0000 0.0000 1.2500
 2 3 9 72.0932 5.0000 1.0000 0.0000 1.0009 0.0000 1.2500
 32 ! Nr of torsions;at1;at2;at3;at4;;V1;V2;V3;V2(BO);vconj;n.u;n
 1 1 1 1 -0.2500 34.7453 0.0288 -6.3507 -1.6000 0.0000 0.0000
 1 1 1 2 -0.2500 29.2131 0.2945 -4.9581 -2.1802 0.0000 0.0000
 2 1 1 2 -0.2500 31.2081 0.4539 -4.8923 -2.2677 0.0000 0.0000
 1 1 1 3 1.2799 20.7787 -0.5249 -2.5000 -1.0000 0.0000 0.0000
 2 1 1 3 1.9159 19.8113 0.7914 -4.6995 -1.0000 0.0000 0.0000
 3 1 1 3 -1.4477 16.6853 0.6461 -4.9622 -1.0000 0.0000 0.0000
 1 1 3 1 0.4816 19.6316 -0.0057 -2.5000 -1.0000 0.0000 0.0000
 1 1 3 2 1.2044 80.0000 -0.3139 -6.1481 -1.0000 0.0000 0.0000
 2 1 3 1 -2.5000 31.0191 0.6165 -2.7733 -2.9807 0.0000 0.0000
 2 1 3 2 -2.4875 70.8145 0.7582 -4.2274 -3.0000 0.0000 0.0000
 1 1 3 3 -0.3566 10.0000 0.0816 -2.6110 -1.9631 0.0000 0.0000
 2 1 3 3 -1.4383 80.0000 1.0000 -3.6877 -2.8000 0.0000 0.0000
 3 1 3 1 -1.1390 78.0747 -0.0964 -4.5172 -3.0000 0.0000 0.0000
 3 1 3 2 -2.5000 70.3345 -1.0000 -5.5315 -3.0000 0.0000 0.0000
 3 1 3 3 -2.0234 80.0000 0.1684 -3.1568 -2.6174 0.0000 0.0000
 1 3 3 1 1.1637 -17.3637 0.5459 -3.6005 -2.6938 0.0000 0.0000
 1 3 3 2 -2.1289 12.8382 1.0000 -5.6657 -2.9759 0.0000 0.0000
 2 3 3 2 2.5000 -22.9397 0.6991 -3.3961 -1.0000 0.0000 0.0000
 1 3 3 3 2.5000 -25.0000 1.0000 -2.5000 -1.0000 0.0000 0.0000
 2 3 3 3 -2.5000 -2.5103 -1.0000 -2.5000 -1.0000 0.0000 0.0000
 3 3 3 3 -2.5000 -25.0000 1.0000 -2.5000 -1.0000 0.0000 0.0000
 0 1 2 0 0.0000 0.0000 0.0000 0.0000 0.0000 0.0000 0.0000
 0 2 2 0 0.0000 0.0000 0.0000 0.0000 0.0000 0.0000 0.0000
 0 2 3 0 0.0000 0.1000 0.0200 -2.5415 0.0000 0.0000 0.0000
 0 1 1 0 0.0000 50.0000 0.3000 -4.0000 -2.0000 0.0000 0.0000
 0 3 3 0 0.5511 25.4150 1.1330 -5.1903 -1.0000 0.0000 0.0000
 1 1 3 3 -0.0002 20.1851 0.1601 -9.0000 -2.0000 0.0000 0.0000
 1 3 3 1 0.0002 80.0000 -1.5000 -4.4848 -2.0000 0.0000 0.0000
 3 1 3 3 -0.1583 20.0000 1.5000 -9.0000 -2.0000 0.0000 0.0000
 2 6 6 2 0.0000 0.0000 0.0640 -2.4426 0.0000 0.0000 0.0000
 2 6 6 6 0.0000 0.0000 0.1587 -2.4426 0.0000 0.0000 0.0000
 0 2 6 0 0.0000 0.0000 0.1200 -2.4847 0.0000 0.0000 0.0000
 1 ! Nr of hydrogen bonds;at1;at2;at3;Rhb;Dehb;vhb1
 3 2 3 2.1200 -3.5800 1.4500 19.5000

F. REFERENCE

- 1 Y. Xiang, J. Du, M. M. Smedskjaer and J. C. Mauro, Structure and properties of sodium aluminosilicate glasses from molecular dynamics simulations, *The Journal of Chemical Physics*, 2013, **139**, 044507.
- 2 J. L. Provis, A. Hajimohammadi, C. E. White, S. A. Bernal, R. J. Myers, R. P. Winarski, V. Rose, T. E. Proffen, A. Llobet and J. S. J. van Deenter, Nanostructural characterization of geopolymers by advanced beamline techniques, *Cement and Concrete Composites*, 2013, **36**, 56–64.
- 3 F. Lolli, H. Manzano, J. L. Provis, M. C. Bignozzi and E. Masoero, Atomistic Simulations of Geopolymer Models: The Impact of Disorder on Structure and Mechanics, *ACS Appl. Mater. Interfaces*, 2018, **10**, 22809–22820.
- 4 S. H. Hahn, J. Rimsza, L. Criscenti, W. Sun, L. Deng, J. Du, T. Liang, S. B. Sinnott and A. C. T. van Duin, Development of a ReaxFF Reactive Force Field for NaSiO_x/Water Systems and Its Application to Sodium and Proton Self-Diffusion, *J. Phys. Chem. C*, 2018, **122**, 19613–19624.
- 5 N. T. Skipper and G. W. Neilson, X-ray and neutron diffraction studies on concentrated aqueous solutions of sodium nitrate and silver nitrate, *J. Phys.: Condens. Matter*, 1989, **1**, 4141–4154.
- 6 M. A. Howe, The hydration of ions in aqueous solution: reverse Monte Carlo analysis of neutron diffraction data, *J. Phys.: Condens. Matter*, 1990, **2**, 741–748.
- 7 R. W. Impey, P. A. Madden and I. R. McDonald, Hydration and mobility of ions in solution, *J. Phys. Chem.*, 1983, **87**, 5071–5083.
- 8 T. Ohkubo, S. Gin, M. Collin and Y. Iwadate, Molecular Dynamics Simulation of Water Confinement in Disordered Aluminosilicate Subnanopores, *Scientific Reports*.
- 9 A. Venkatnathan, R. Devanathan and M. Dupuis, Atomistic Simulations of Hydrated Nafion and Temperature Effects on Hydronium Ion Mobility, *J. Phys. Chem. B*, 2007, **111**, 7234–7244.
- 10 S. Cui, J. Liu, M. E. Selvan, D. J. Keffer, B. J. Edwards and W. V. Steele, A Molecular Dynamics Study of a Nafion Polyelectrolyte Membrane and the Aqueous Phase Structure for Proton Transport, *J. Phys. Chem. B*, 2007, **111**, 2208–2218.
- 11 S. Urata, J. Irisawa, A. Takada, W. Shinoda, S. Tsuzuki and M. Mikami, Molecular Dynamics Simulation of Swollen Membrane of Perfluorinated Ionomer, *J. Phys. Chem. B*, 2005, **109**, 4269–4278.
- 12 M. Chen, H.-Y. Ko, R. C. Remsing, M. F. C. Andrade, B. Santra, Z. Sun, A. Selloni, R. Car, M. L. Klein, J. P. Perdew and X. Wu, Ab initio theory and modeling of water, *PNAS*, 2017, **114**, 10846–10851.
- 13 S. H. Hahn and A. C. T. van Duin, Surface Reactivity and Leaching of a Sodium Silicate Glass under an Aqueous Environment: A ReaxFF Molecular Dynamics Study, *J. Phys. Chem. C*, 2019, **123**, 15606–15617.
- 14 N. M. A. Krishnan, B. Wang, G. Falzone, Y. Le Pape, N. Neithalath, L. Pilon, M. Bauchy and G. Sant, Confined Water in Layered Silicates: The Origin of Anomalous Thermal Expansion Behavior in Calcium-Silicate-Hydrates, *ACS Applied Materials & Interfaces*, 2016, **8**, 35621–35627.
- 15 N. M. A. Krishnan, B. Wang, G. Sant, J. C. Phillips and M. Bauchy, Revealing the Effect of Irradiation on Cement Hydrates: Evidence of a Topological Self-Organization, *ACS Applied Materials & Interfaces*, 2017, **9**, 32377–32385.
- 16 A. K. Soper, The radial distribution functions of water and ice from 220 to 673 K and at pressures up to 400 MPa, *Chemical Physics*, 2000, **258**, 121–137.